VIBRATIONAL ENERGY REDISTRIBUTION ACROSS A HEAVY ATOM

Steven M. LEDERMAN ^{a,1}, Vicente LÓPEZ ^b, Victor FAIRÉN ^c, Gregory A. VOTH ^{a,2} and R.A. MARCUS ^a

- a Arthur Amos Noyes Laboratory of Chemical Physics³, California Institute of Technology, Pasadena, CA 91125, USA
- b Departamento de Química, Universidad Autónoma de Madrid, 28049 Madrid, Spain
- c Departamento de Física Fundamental, Universidad Nacional de Educación a Distancia, Apdo. 60141, 28080 Madrid, Spain

Received 11 May 1989

Vibrational energy relaxation is studied for a model system with two different ligands separated by a heavy atom, there being initially an excess energy in one metal-ligand subsystem. The model has eleven coordinates to achieve a high density of states (two coordinates for one metal-ligand subsystem and nine for the other). The behavior was studied using classical and quantum mechanical methods, and the results compared. Artificial intelligence searching was used in the quantum treatment, because of the large number of potentially contributing quantum states. For the present system the adiabatic separation of motion of the local group modes, previously characterized for a C-C-Sn ligand in a smaller system, still holds when the other ligand has this high density of states. Further, the agreement between the classical and quantum results is much improved over that obtained earlier for a four-coordinate symmetric system. In the latter case isolated intrinsic resonances were responsible for the "energy transfer", which was facilitated sometimes by tunneling. The present agreement of the classical and quantum calculations is generally quantitative at shorter times and at least qualitative for longer times for most states studied. This agreement is encouraging since the former can be less computationally intensive.

1. Introduction

In previous papers [1-3] we considered model systems containing two identical ligands separated by a heavy atom, there being four coordinates in all. The ligands were treated as linear carbon skeleton chains and the heavy central atom was tin. These models were initially motivated by an experimental study [4] that suggested the possibility that a central tin atom acted as a barrier which reduced the rate of intramolecular vibrational energy transfer between hydrocarbon ligands. Subsequent experiments [5,6] on related chemical systems gave a contradictory conclusion. Large classical calculations on a model related to the experimental molecules led to results which showed a dependence of the potential energy surface used [7].

- Present address: Supercomputing Research Center, 17100 Duckett Drive, Bowie, MD 20716, USA.
- Present address: Department of Chemistry, University of Pennsylvania, Philadelphia, PA 19104-6323, USA.
- ³ Contribution No. 7929.

In our previous theoretical studies on a small system (two coordinates for each metal-ligand subsystem) it was found that the motion of ligands attached to a heavy atom could be described with what was termed local group modes [1]. Each of the latter involved an anharmonic collective motion of the metal and the ligand atoms attached to it and they resulted in the approximate constants of the motion. The quantum state for a metal-ligand subsystem was described using semiclassical theory, by specifying the relevant actions and, thereby, semiclassically the corresponding quantum numbers. These local group modes characterized separate motions of the ligand and the heavy atom attached to it, independently of the rest of the molecule, in the same way a local mode characterizes the motion of a light atom attached to a molecule by a relatively heavier atom [1-3]. For the system studied, both the classical and the quantum calculations on a linear model system confirmed the presence and usefulness of the local group mode concept in describing the dynamics of such systems.

A system composed of ligands separated by a heavy

atom can be viewed as a perturbation of the limiting case in which an infinite central mass leads (in the absence of potential energy coupling) to an independent motion of the ligands. Resonances between metal-ligand subsystems are responsible for strong modifications of the dynamics of the ligands for a finite central mass and can lead to vibrational energy transfer between the ligands [1-3,8]. The symmetric model systems used in our previous studies [2,3] (e.g., C-C-Sn-C-C) resulted in the existence of a 1:1 resonance that was intrinsic and therefore present for all energies of excitation. The local group mode concept yielded physical insight into the dynamics of different excitations of the ligands. For the case of a C-C-Sn ligand and adiabatic separability of the two local group modes led to completely different dynamics when the different local group modes were excited [1-3]. The results of these studies were instructive, but the symmetry of the model meant that experimentally the studies would be more related to spectroscopic splittings between symmetric and asymmetric states rather than to the study of real-time energy redistribution.

In this paper, energy transfer is studied in a nonsymmetric model system with two different ligands separated by a heavy atom and so the results are more closely related to real-time energy redistribution. One ligand is the previously characterized C-C-Sn chain while the other ligand is a model for a higher-dimensional deuterium-substituted carbon chain. We have used an artificial intelligence searching method [9] to calculate the quantum mechanical time evolution and loss of the energy in an excited C-C-Sn moiety. These quantum results are compared to results for the time evolution obtained using classical or partly semiclassical methods. The results of the present study show that the adiabatic separation of motion of the two local group modes found in our previous study for the C-C-Sn subsystem still occurs and that resulting differences in the energy transfer can be distinguished. The results also permit a comparison of quantum and classical calculations for this larger system.

The model system used in the present study is discussed in section 2. A description of the classical and quantum calculations is given in section 3. The results are given in section 4 and discussed in section 5.

2. Model system

In order to test the effectiveness of the adiabatic separation of the motion of the local group modes of the two degree-of-freedom-ligand subsystem found previously [2,3], the C-C-Sn chain was retained as one of the ligands attached to the heavy atom. To make the model closer to molecules of experimental interest (and to relate to a real-time evolution), the number of coordinates in the second ligand was increased, thereby introducing an asymmetry of the ligands.

The increase in the number of degrees of freedom causes an increase in the density of states [10] which is shown to be strongly correlated to the amount of relaxation in the model system. The increase in the number of degrees of freedom and the asymmetry can be achieved by mimicking a common experimental technique for labelling, e.g., isotope substitution. With this in mind the previous five-atom model was modified, in part, by mass-weighting the carbons to effectively include the masses of hydrogen in one ligand and deuterium in the other ligand. The number of degrees of freedom in the deuterated ligand was also increased, by considering explicitly the motions of two deuterium atoms and all bending motions. The resulting model could still be treated reliably with both quantum and classical mechanics and provides some insight on energy transfer across a heavy atom.

In the present paper an eleven-degree-of-freedom dynamical system, intended as a step toward modelling a larger system, $(CH_3CH_2)_3SnCD_2CD_3$, is discussed and depicted in fig. 1. One ligand subsystem, C-C-Sn, denoted by L₁ below, is similar to the ligand previously studied in the symmetric model in which only the two vibrational stretching motions were considered, except that in the present ligand the carbon chain is not linear but is chosen to have the ex-

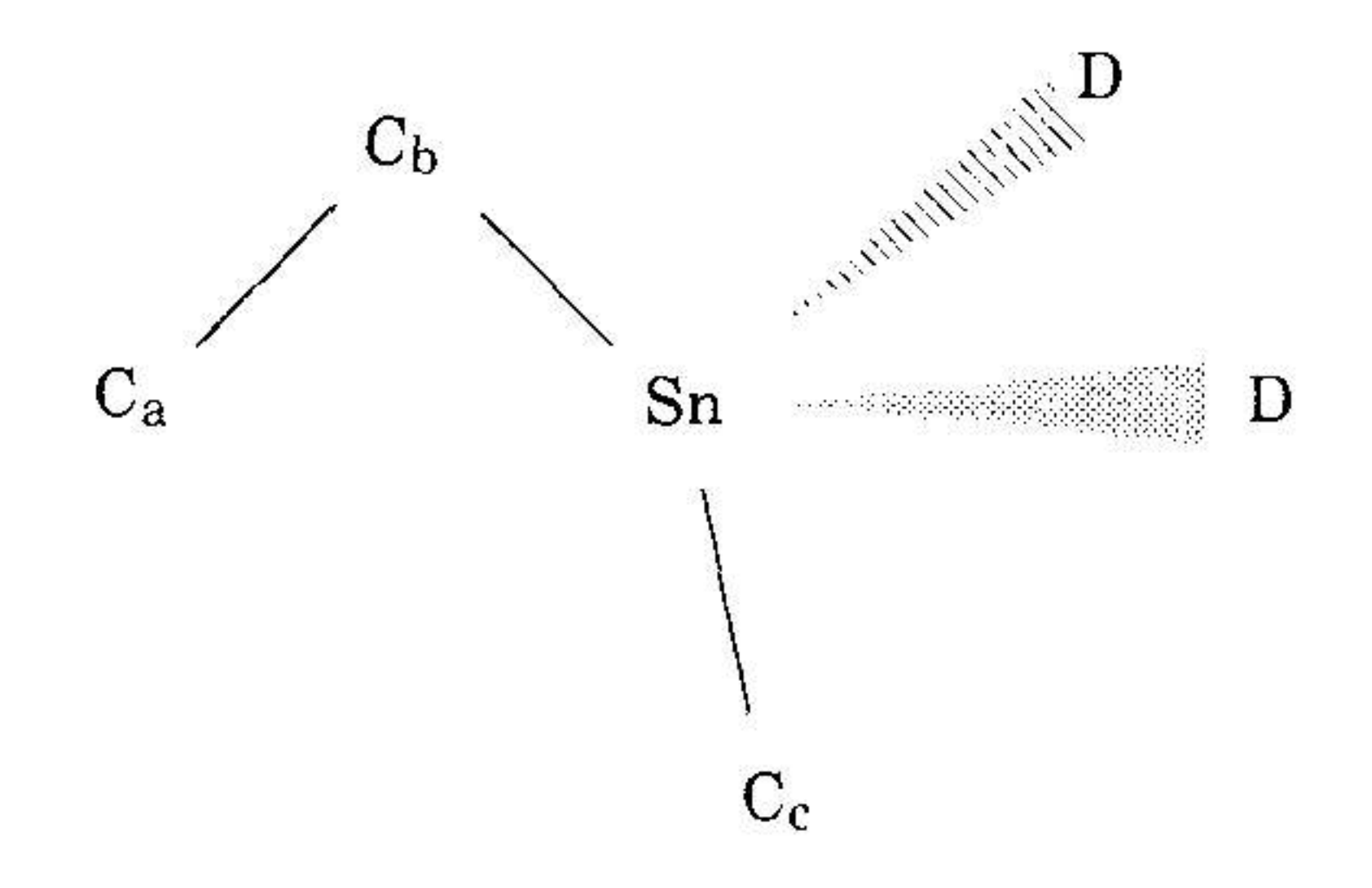


Fig. 1. Model system studied. $L_1 = C_a C_b Sn$, $L_2 = Sn(D)_2 C_c$.

perimental tetrahedral angles. The second ligand-metal subsystem, denoted by L₂, has nine vibrational degrees of freedom, namely, the four stretching and five bending motions associated with a methane-like ligand [11]. The carbon atoms labeled C_a, C_b and C_c in fig. 1 were given the effective masses of CH₃, CH₂ and CD₃, respectively, to simulate the mass of the attached atoms not included explicitly *1. The Hamiltonian chosen for this model system is

$$H = H_1 + H_2 + V_{12} \,, \tag{1}$$

where

$$H_1 = \frac{1}{2} \sum_{i=1}^{2} \sum_{j=1}^{2} p_i G_{ij} p_j$$

$$+ \sum_{i=1}^{2} D_i \{1 - \exp[\alpha_i(q_i - q_i^e)]\}^2, \qquad (2)$$

$$H_2 = \frac{1}{2} \sum_{i=3}^{12} \sum_{j=3}^{12} \left[p_i \left(G_{ij} + \sum_{k=3}^{12} \frac{\partial G_{ij}}{\partial q_k} \bigg|_{q=q^e} q_k \right) p_j \right]$$

$$+\frac{1}{2}\sum_{i=3}^{12}k_i(q_i-q_i^e)^2, \qquad (3)$$

$$V_{12} = \lambda (p_2 p_3 \cos \theta^e) / M$$
. (4)

Here, q_i and p_i are the internal coordinates and their conjugate momenta, respectively, and q_i^e is the equilibrium value of the *i*th bond coordinate given in table 1. The G_{ij} are the Wilson G matrix elements [11] and are evaluated, together with their first derivatives, at the equilibrium value of the bond coordinates. This H_2 represents a two-term expansion of the actual coordinate dependent kinetic energy matrix element. θ^e in eq. (4) is the equilibrium tetrahedral angle C-Sn-C between the two ligands. Analytic expressions for the first derivatives of the G matrix with respect to the displacement coordinates were obtained using the symbolic manipulation pro-

Table 1
Parameters of model Hamiltonian

	D a) (kcal/mole)	$\alpha^{b)}$ (Å ⁻¹)		
C_a - C_b	84.08	1.8194		
C_b -Sn	52.84	1.6426		
Bond	Equilibrium			
	distance	$eq^{ec}(A)$		
Sn-C	2.143			
C-D	1.093			
$C-C_c$	1.552			
Bond		Force		
		constant c)		
Sn-C		$k_{rr} = 1.5858$		
C-D		$k_{rr} = 4.72$		
$C-C_c$		$k_{rr} = 4.76$		
Sn-C-D		$k_{\theta\theta} = 0.74$		
$Sn-C-C_c$		$k_{\theta\theta} = 0.65$		
$D-C-C_c$		$k_{\theta\theta} = 0.62$		
D-C-D		$k_{\theta\theta} = 0.46$		
$Sn-C/C-C_c$	į	$k_{rr'} = -0.28$		
D. 0, 0 0	•			

a) Ref. [12]. b) Ref. [13].

gram *2, which was also used to provide the Fortran expressions.

The set of ten bond coordinates included in H_2 in eq. (3) contains a redundant bending coordinate [11], since the sum of all the displacement angles is constrained to be a constant value. This redundant variable is one of the ten symmetry coordinates. For this reason H_2 was transformed into symmetry coordinates before performing the classical and quantum evolutions. The values of the Morse parameters D_i and α_i , for L₁ are given in table 1. The anharmonicity parameters α_i , in eq. (2), were obtained from the harmonic limit of the Morse oscillator where $\alpha_i = \sqrt{f_i/2D_i}$, and the f_i are the harmonic force constants. A non-linear least-squares fit of the normal mode frequencies in terms of the bond mode force constants to the experimental frequencies [15] was performed to determine the harmonic force constants f_i .

The values used are for the average mass weighted by the natural abundance. The mass (in g/mole) of Sn equals 118.69, C equals 12.01115, D equals 2.014, C_a (\equiv CH₃) equals 15.03506, C_b (\equiv CH₂) equals 14.027109, and C_c (\equiv CD₃) equals 18.0532.

c) Ref. [14]. k_{rr} and $k_{rr'}$ in mdyn/Å, $k_{\theta\theta}$ in mdyn Å and $k_{r\theta}$ in mdyn.

^{*2} SMP was developed by the High Energy Physics Group at Caltech.

In the case of the ligand-metal subsystem L_2 , the harmonic force constants k_i were determined from the literature [14] where the experimental frequencies of $CH_2CH_3SnH_3$ molecule were analyzed. In order to translate those values to our approximate molecular mode, the Sn-C force constant for L_2 was optimized until agreement was obtained with the experimental frequency for the predominantly Sn-C normal mode. To be able to compare the present model with the experimental frequencies, the deuterium atoms in L_2 were replaced with hydrogen atoms during the optimization. The force constants determined in the above manner were then used in the deuterated model given in fig. 1 and are tabulated in table 1.

To test the utility of the first-order approximation to the G matrix dependence on the displacements, we have also evaluated classically the dynamics generated by a more general Hamiltonian for the ligand metal L_2 ,

$$H_2 = \frac{1}{2} \sum_{i=3}^{12} \sum_{j=3}^{12} p_i G_{ij}(\mathbf{q}) p_j + \frac{1}{2} \sum_{i=3}^{12} k_i (q_i - q_i^e)^2, \qquad (5)$$

where the complete dependence of the G_{ij} on the displacement of \boldsymbol{q} is included.

The Hamiltonian for L_1 contains Morse potentials, in order to retain the local group modes discussed in the previous papers [1-3]. The Hamiltonian for L_2 has harmonic potentials, but the first derivative of the G matrix elements adds cubic anharmonic couplings [16]. Further, the first derivatives of the G matrix remove the symmetry-based decoupling of the three A' modes in L₂ from the remaining modes of the molecule, i.e. both L₁ and L₂. Harmonic potentials were used for L2, and the necessary quantum matrix elements were easily calculated, as discussed below. The coupling between L₁ and L₂ is represented as a kinetic coupling in the present model. The kinetic coupling between L₁ and L₂ depends on the central mass (M in eq. (4)), and the effect of varying that central mass on the energy transfer is studied below.

However, varying the central mass not only affects the kinetic coupling term but also changes the frequencies associated with each ligand. A change in the frequencies of the ligands can cause changes in the energy transfer between these ligands by modifying the resonances between them. Since the model only crudely approximates actual molecular systems, only the general trends expected from varying the central mass will be studied here. By varying, instead, the parameter λ in eq. (4) a change in the kinetic coupling between the ligands associated with a change in the central mass could be mimicked without varying the frequencies of the metal-ligand subsystems. In this way the two effects of varying M were separated. The central mass M is set equal to that of tin in the present study and the parameter λ is varied to change the value of the coupling term between the L_1 and L_2 to the values associated with a series of central masses. Thus, a "pure" mass effect upon energy transfer was studied without the effect of having a change in vibration frequencies.

3. Dynamic description

The flow of energy across the heavy atom in the present model was examined for different initial excitations using both classical and quantum mechanics. The initial states of the model system were characterized using the pair of quantum numbers of the local group modes of L₁ and the nine quantum numbers of the zeroth-order harmonic normal modes of L₂. The local group modes were those characterized for a similar L₁ in a previous study [2]. At very low excitation energies they practically coincide with the two normal modes of the ligand, whereas for higher excitation energies the high-frequency mode corresponds predominantly to the C-C stretching (i.e. to the vibration of the C against C-Sn) and the other to the stretching of the C-C group against the Sn atom. For this reason the high-frequency local group mode in L₁ will be referred to as the C local group mode with quantum number $n_{\rm C}$ and the low-frequency mode as the Sn local group mode with quantum number $n_{\rm Sn}$ #3. The flow of energy across the central heavy atom is induced by the presence of the V_{12} term in the full Hamiltonian dynamics based on eq. (1).

The semiclassical adiabatic switching method [17] was used to obtain the tori for the classical quasi-periodic motion of L_1 with actions, J_C and J_{Sn} of the local group modes for the Hamiltonian of L_1 . The latter were chosen for given n_C and n_{Sn} from the EBK

^{#3} In refs. [2,3] the C and Sn local group modes were referred to as X and Y modes, respectively.

semiclassical relations, $J_C = (n_C + 1/2)h$, $J_{Sn} = (n_{Sn} + 1/2)h$. The zeroth-order actions of L_1 were chosen to be the normal mode actions in the harmonic limit of the Morse oscillators, and the anharmonicities were switched on during periods of time longer than 200 times the period of the higher-frequency normal mode. Converged values of the energy in the final perturbed torus were obtained for excitations lower than 8000 cm⁻¹. Above this energy the instabilities of the results suggested the presence of resonances between the two degrees of freedom of L_1 . Only excitations below this limit have been used as initial states in the present dynamical studies.

The semiclassical results were also used for the labeling of the quantum mechanical wavefunctions for L₁. These wavefunctions for the L₁ ligand were obtained by diagonalization of H_1 using a basis set of 1497 elements, consisting of the products of Morse oscillator wavefunctions. The basis set included in the calculation contained all elements with a total energy less than 28000 cm⁻¹. This procedure provided converged results for all the L₁ wavefunctions used in the dynamics. Comparison between the energies obtained in the diagonalization and the energies of phase space points on the semiclassical tori permitted the latter to be used in the labeling of the L₁ wavefunctions in terms of local group modes. The values of the energies obtained semiclassically were almost always close enough to the quantum eigenvalues of H_1 to allow a unique assignment of the pair of quantum numbers $(n_{\rm C}, n_{\rm Sn})$ to the wavefunctions.

For every initial excitation of the system considered, Hamilton's equations of motion were integrated for a set of 25 initial conditions randomly chosen from those on the semiclassical zeroth-order torus labeled with the specified set of the eleven quantum numbers. The ligand L₂ contained the zero-point energy of the nine modes. The excess energy E_1 in L_1 , at any time step was defined classically as the average of the function H_1 in eq. (1) over the 25 trajectories, minus the quantum zero-point energy in L₁. While this average over the set of initial conditions on the initial unperturbed torus for the Hamiltonian H_1+H_2 , provides a better correspondence to the quantum time evolution of the expectation value of the operator \hat{H}_1 than the consideration of single trajectories, the high dimensionality of the phase space would normally require a very large representative

sampling of the phase space. An average over 25 trajectories provided a coarse graining over some of the irrelevant single trajectory oscillations and so permitted a better comparison with the quantum results.

For the quantum dynamics, the basis set wavefunctions used were the product of the wavefunctions of H_1 with the normal mode wavefunctions of L_2 . The latter were the eigenfunctions of H_2 when the first derivatives of the G matrix are omitted. In this basis set there are two types of off-diagonal matrix elements of the Hamiltonian given in eq. (1) that need to be evaluated, namely, those arising from the first derivatives of the G matrix and those due to the V_{12} coupling between L_1 and L_2 . The latter are the more difficult to evaluate. Thus, to obtain the V_{12} matrix elements the eigenfunctions of H_1 were expressed in terms of the original local mode Morse oscillator wavefunctions. This transformation was computationally intensive and required almost 10 min of CPU time on a Cray-2 to determine the momentum matrix elements for the 101 lowest energy wavefunctions of L₁. The lowest 101 wavefunctions of L₁ were the the ones used in the dynamics of the complete system. The transformation, however, needed only to be performed once for a given choice of parameters.

Since L_2 has nine degrees of freedom, the basis set of L_2 was chosen to avoid the necessity of making a numerical transformation of coordinates in order to evaluate the V_{12} matrix elements. This procedure is possible with the use of a normal mode basis set for which there exists a linear transformation from local bond coordinates into normal mode coordinates *4. The latter transformation permitted the ready evaluation of the V_{12} matrix elements in the normal modes basis set.

The basis set elements used in the quantum calculation of the stationary states of the combined system were determined by the artificial intelligence (AI) best-first search, which has been discussed in detail elsewhere [9]. In using this method the possible a priori basis elements were searched to find those members of the basis set which are important for the

^{#4} It is noted that one of the symmetry coordinates coincides with the local mode coordinate for the Sn-C bond in L₂ so that transformation from the normal mode coordinates into symmetry coordinates trivially yields the Sn-C local bond mode.

subsequent dynamics of time evolution from a selected initial excitation. The best-first search method was used in the present calculations because the high dimensionality of the model presented would have required consideration of numerous basis states if all basis states within the energy range of the initial state were considered. For example, one excitation of the present model at 7000 cm⁻¹ of excess energy would have required the inclusion of over 64000 basis set functions if all basis set states within twice the energy spread of the initial state wavefunction were included. Such a number of basis states would pose a formidable problem for calculating the dynamics in a reasonable amount of computer time.

Application of the AI best-first search considerably reduced the number of states necessary for performing the dynamics without strictly restricting the energy range of basis set states considered or excluding more degrees of freedom. Another advantage of using the AI best-first search for determining the important dynamical states is that the amount of computer time required for performing the dynamics on higher energy excitations is comparable to lower energy excitations even though the density of states increases exponentially. For example, an excess energy excitation of the L_1 of 7108 cm⁻¹ required 18 min of VAX 11/780 CPU time to perform the AI best-first search for 1000 basis functions, while an excitation of 3855 cm⁻¹ required 15 min. Thus, the higher energy excitation required only 20% more computer time for the AI best-first search even though the excess energy was almost double and the density of states was over 40 times greater. Further, the computer time spent on the AI best-first search was less than one percent of the computer cost necessary to perform the dynamics.

In the results presented, the AI best-first search method was used to choose 1000 basis states with no restriction on their energy. The eigenstates of the full Hamiltonian in eq. (1) were determined on this restricted basis set by performing a matrix diagonalization. Each initial state chosen in the present calculations was an element of the basis set used to determine the eigenstates of the system. The time evolution of the initial state was approximated by the time evolution of the appropriate linear combination of eigenstates. The dynamical quantity calculated was the excess energy in L_1 as a function of time (in ex-

cess of the zero-point energy), given by calculating at each time the expectation value of H_1 for the propagated initial excitation of the system. The dynamics was performed using the selected 1000 basis set states, since it was found that the dynamical quantity $E_1(t)$, the excess energy in L_1 at time t, was "converged" at the time studied for this number of basis set states using the AI best-first search method.

4. Results

Previous results for the classical and quantum time evolutions for the two-degree-of-freedom subsystem L₁, e.g., C-C-Sn, coupled to a similar subsystem L₂ in a symmetric model system showed an adiabatic separation of motion of what we have termed here C and Sn local group modes [1-3] *3. The analysis given below of the time evolution of the present model system indicates that the adiabatic separation of motion of the C and Sn local group modes found in refs. [1– 3] remains when the C-C-Sn subsystem L₁ is coupled instead to the high-dimensional ligand of the present model. This result justifies the description of the energy transfer in the present model system in terms of these local group modes excitations, since the different excitations show qualitatively different behavior in the amount of energy transferred to L_2 , which initially had only zero-point energy. This result may be seen in fig. 2, where the time evolution of E_1 is given for initial excitations of both modes. These quantum calculations confirm the previous results [2,3], in which for a C local group mode excitation $(n_C=8, n_{Sn}=0, \text{ in fig. 2})$ there is a localization of the excess energy on L₁, while an excitation of the Sn local group mode ($n_C=0$, $n_{Sn}=15$, in fig. 2) is identified as responsible for the excess energy loss from the C-C-Sn system. For the comparison, both initial excitations were chosen to be close in energy ($\Delta E = 28$ cm^{-1}).

In fig. 3 a plot of the excess energy E_1 in L_1 versus time is given for a series of increasing excitations for both pure C and Sn local group modes. It can be seen that while the excitation of a C local group mode does not produce a significant transfer of energy for a series of excitations between the (4,0) and (8,0) states $(3688 \text{ to } 7141 \text{ cm}^{-1})$, the excitation of a Sn local group mode yields an increase in the amount of en-

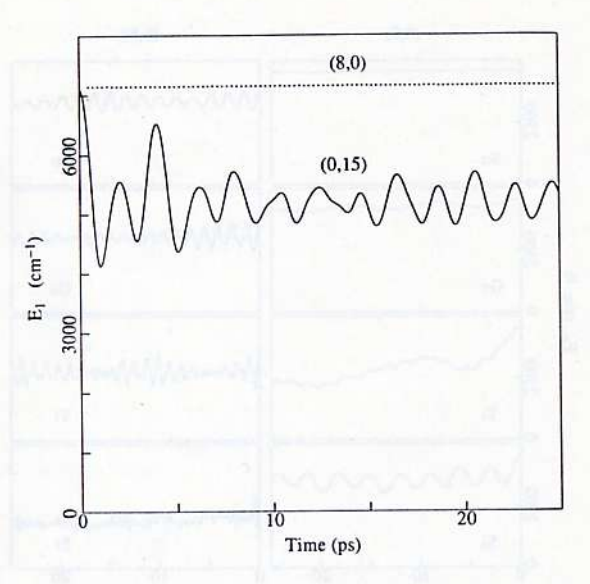


Fig. 2. Comparison of pure C and Sn local group modes with the central mass of Sn for the quantum calculation. The excess energy E_1 in ligand L_1 , is plotted versus time. The solid line arises from an initial excitation of the Sn (0, 15) local group mode and the dotted line from that of the C (8, 0) local group mode.

ergy transfer with increasing excitation energies for the range of the (0, 8) to (0, 15) states (3855 to 7109 cm⁻¹). A quantitative measure of the amount of the energy transfer in the present model system is the percentage of relaxation, R_{96} , which is plotted in fig. 4 versus the excitation energy of L_1 for the pure Sn local group mode excitation. Here, R_{96} is defined as

$$R_{\%} = [1 - \langle E_1 \rangle_{\infty} / E_1(t=0)] \times 100,$$
 (6)

where $\langle E_1 \rangle_{\infty}$ is the average energy of L₁ for long times and $E_1(t=0)$ is the initial excitation energy of L₁. All excitations are of L₁ in this study. For the results given in fig. 4, $\langle E_1 \rangle_{\infty}$ is the value of $\langle E_1 \rangle$ found directly from the eigenvalues and eigenvectors in the limit of $t \to \infty$.

It is also interesting to investigate the dependence of the energy transfer upon the magnitude of the kinetic energy term coupling L_1 to L_2 . The parameter λ in eq. (4) has been varied so as to cover a range of couplings simulating the central masses of Sn (λ =1.0), Ge (λ =1.6351), Ti (λ =2.4779), and Si (λ =4.2259) *1. In fig. 5, E_1 is plotted versus time for the (5, 0) and (0, 8) initial excitations for each of the masses specified above. The amount of energy

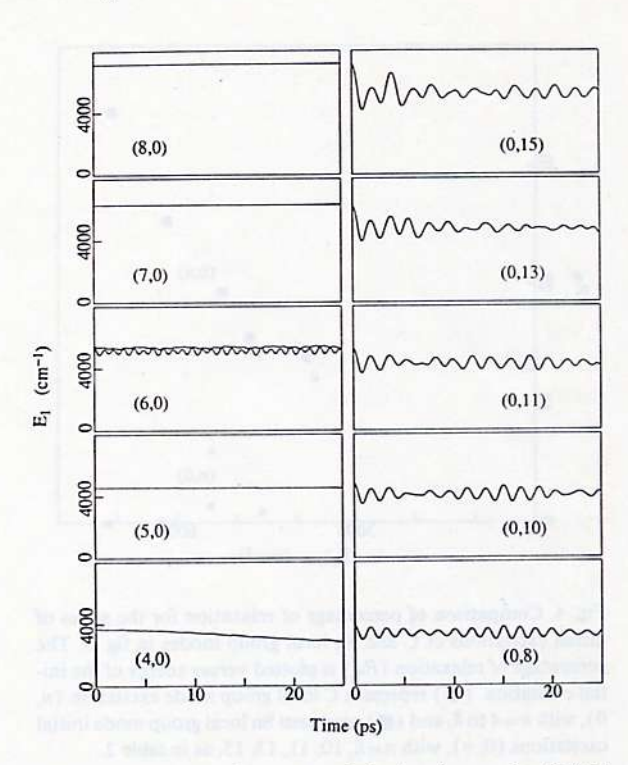


Fig. 3. Comparison of quantum calculations for a series of initial excitations for pure C and Sn local group modes with the central mass of Sn. The series of plots on the left-hand side of the figure are for an initial excitation of the C local group mode whereas the right-hand side is for that of the Sn local group mode. The energy of the initial excitation decreases from the top plot to the bottom plot. The plots across from each other represent C and Sn local group modes of approximately the same energy of initial excitation. The energy E_1 in ligand L_1 is plotted versus time.

transferred displayed in fig. 5 shows the expected decrease with increasing central mass. The percentage of relaxation $R_{\%}$ versus the parameter λ is given in fig. 6 for both the (5,0) and (0,8) excitations.

It is also interesting to compare the classical and quantum estimates of the energy redistribution across the central atom. For symmetric model systems these two sets of results were [1-3] qualitatively different for the amount of energy present in one ligand. The case is different for the present asymmetric model system. In fig. 7 the classical and quantum time evolution of E_1 is compared for the initial excitation (8,0) and the central mass of Sn. Both results agree in showing that the excitation energy remains localized in L_1 . For the Sn local group mode pure excitation (0,15) and the central mass of Sn, both the classical mass

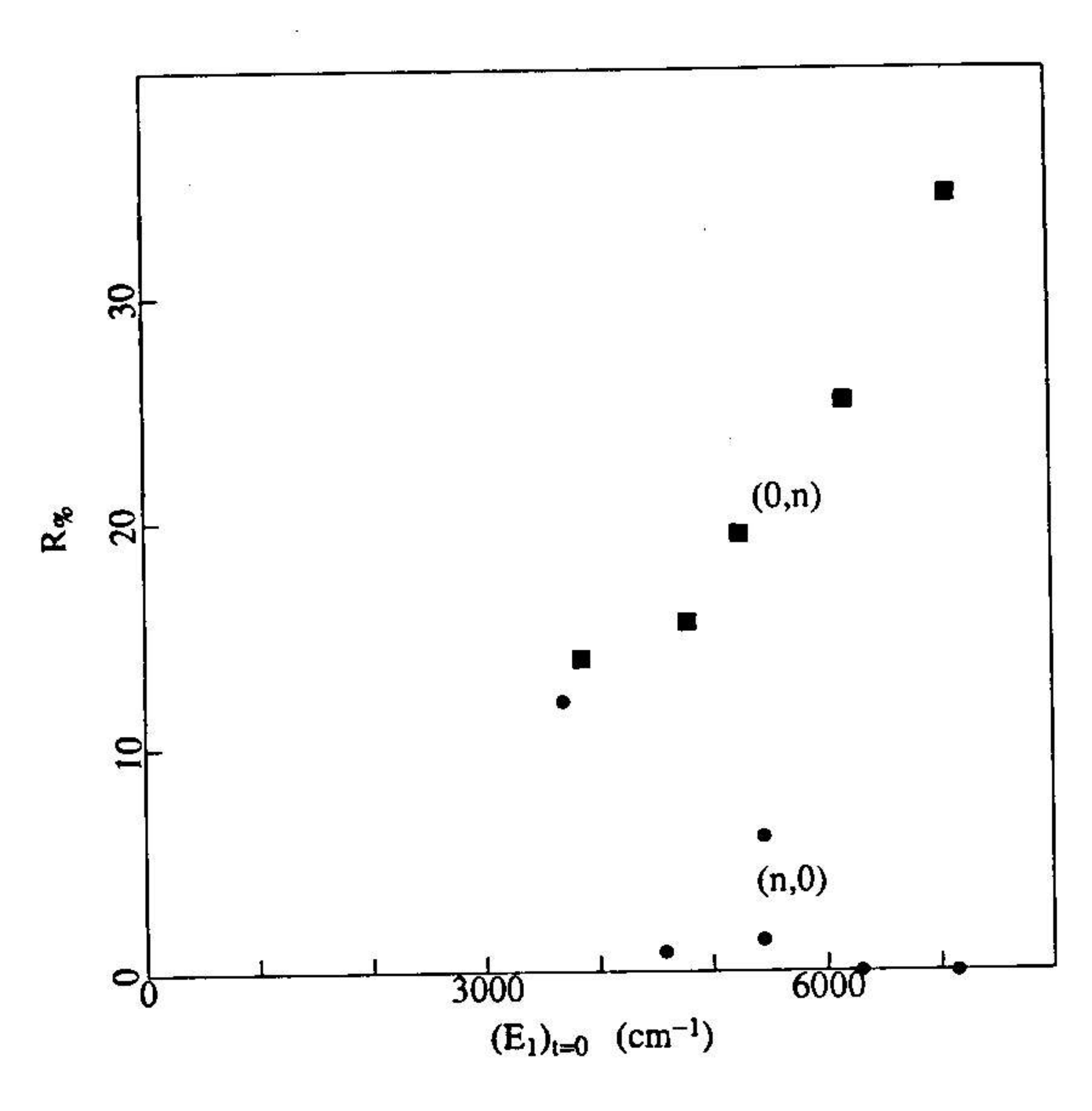


Fig. 4. Comparison of percentage of relaxation for the series of initial excitations of C and Sn local group modes in fig. 3. The percentage of relaxation $(R_{\%})$ is plotted versus energy of the initial excitation. (\bullet) represent C local group mode excitation (n, 0), with n=4 to 8, and (\blacksquare) represent Sn local group mode initial excitations (0, n), with n=8, 10, 11, 13, 15, as in table 2.

sical and quantum time-evolution display in fig. 8 a decay of the energy in L_1 . For some cases, e.g., the (5,0) excitation with Ti, Ge and Si as central mass, we have observed that classical and quantum situations were qualitatively different in their time evolution of the excess energy $E_1(t)$ in L_1 . In fig. 9 the results obtained for Si are shown.

In table 2 the percentage of relaxation $R_{\%}$ is compared for the classical and quantum calculations for all results presented. The classical and first quantum results are from an average of the energy in L_1 from the dynamical calculations from 2 ps to the length of the classical trajectory (generally 10 ps). The second quantum result is that obtained directly from the eigenvalues and eigenvectors when $t\rightarrow\infty$. (The cross terms between wavefunctions vanish in this limit.) The last column is the statistical value as derived in the appendix, eq. (A.4). It represents a semiclassical estimate, assuming separability of the motion of L_1 from that of L_2 , as well as an equal probability for all states in the system.

In the present model system we have included anharmonic terms in the Hamiltonian of L_2 by considering the first-order correction to the variation of the

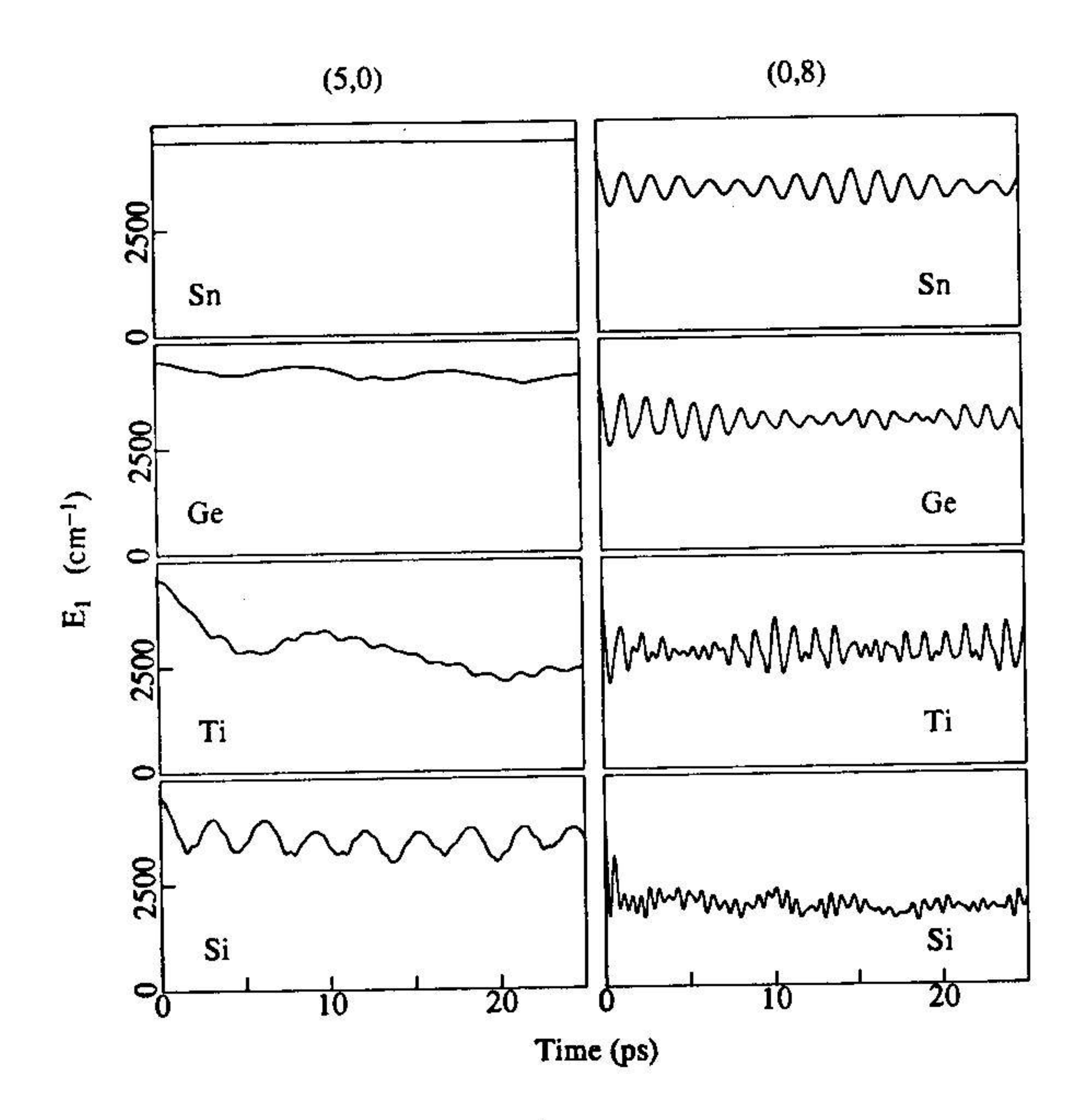


Fig. 5. Comparison of quantum calculations for a series of central masses for C and Sn local group modes. The series of plots on the left-hand side of the figure is for the C (5,0) local group mode initial excitation whereas the right-hand side is for an initial excitation of the Sn (0,8) local group mode, which is similar in energy. The central mass decreases (i.e. λ increases) from the top plot to the bottom plot. The energy E_1 in ligand L_1 is plotted versus time. (λ =effective reciprocal mass parameter in eq. (4).) For Si (0,8) E_1 (t=0)=3855 cm⁻¹, as in table 2.

G matrix with the displacement coordinates. The firstorder correction was used because inclusion of the full G matrix dependence is more difficult to implement in the quantum calculation. (It is even computationally intensive in the classical calculation.) Clearly, this first-order correction is only valid for small displacements from the equilibrium position. To check the effect of higher-order corrections on the energy redistribution across the heavy atom we have studied the classical dynamics of the present model system using H_2 in eq. (5), where the complete dependence of the G matrix on the displacement coordinates is taken into account. The results obtained for the time evolution of E_1 are shown in figs. 7 and 8, for comparison with the results obtained with only the first-order correction to the equilibrium G matrix.

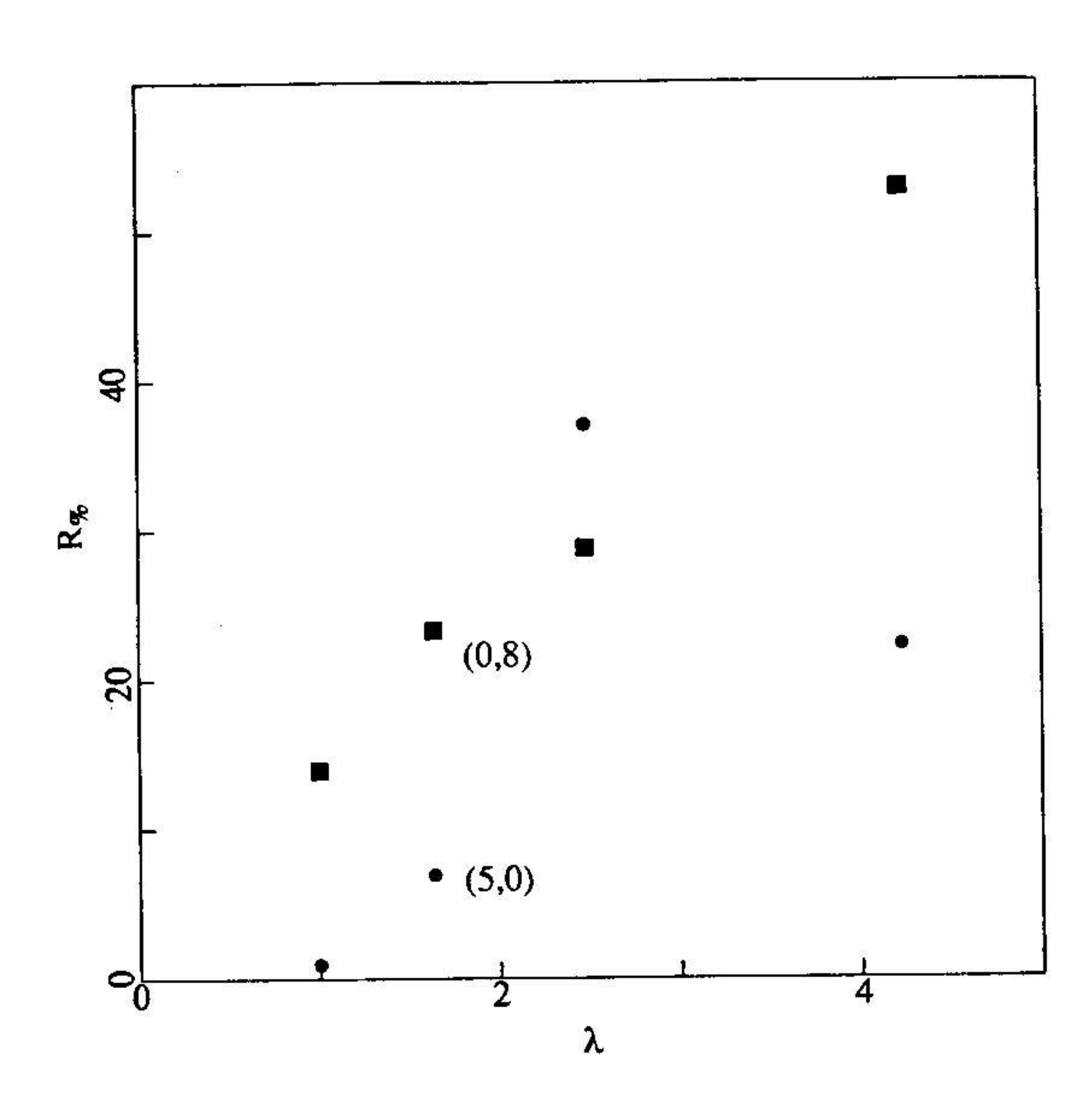


Fig. 6. Comparison of percentage of relaxation for the series of masses in fig. 5 for initial excitation of the C and Sn local group modes. The percentage of relaxation $(R_{\%})$ is plotted versus λ (see text). (\bullet) represent C local group mode excitations and (\blacksquare) represent Sn local group mode excitations.

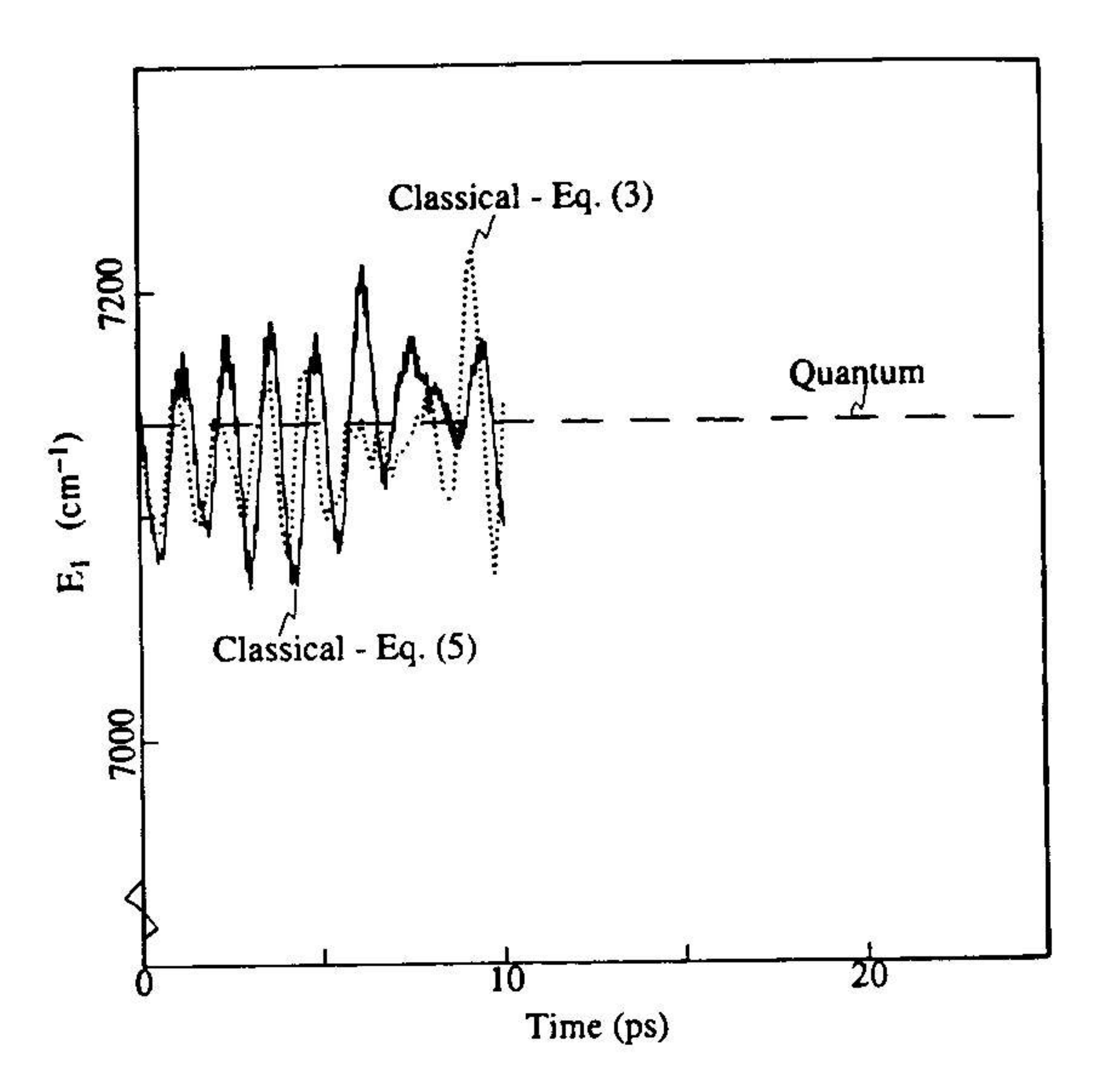


Fig. 7. Comparison of typical quantum and classical calculations for the C (8,0) local group mode initial excitation when the central mass is that of Sn. The energy E_1 in L_1 is plotted versus time. The dashed line represents the quantum calculation, the dotted line the classical calculation using for L_2 the Hamiltonian H_2 in eq. (3) and the solid line the analogous classical calculation using the Hamiltonian H_2 in eq. (5). Note that the y axis is broken.

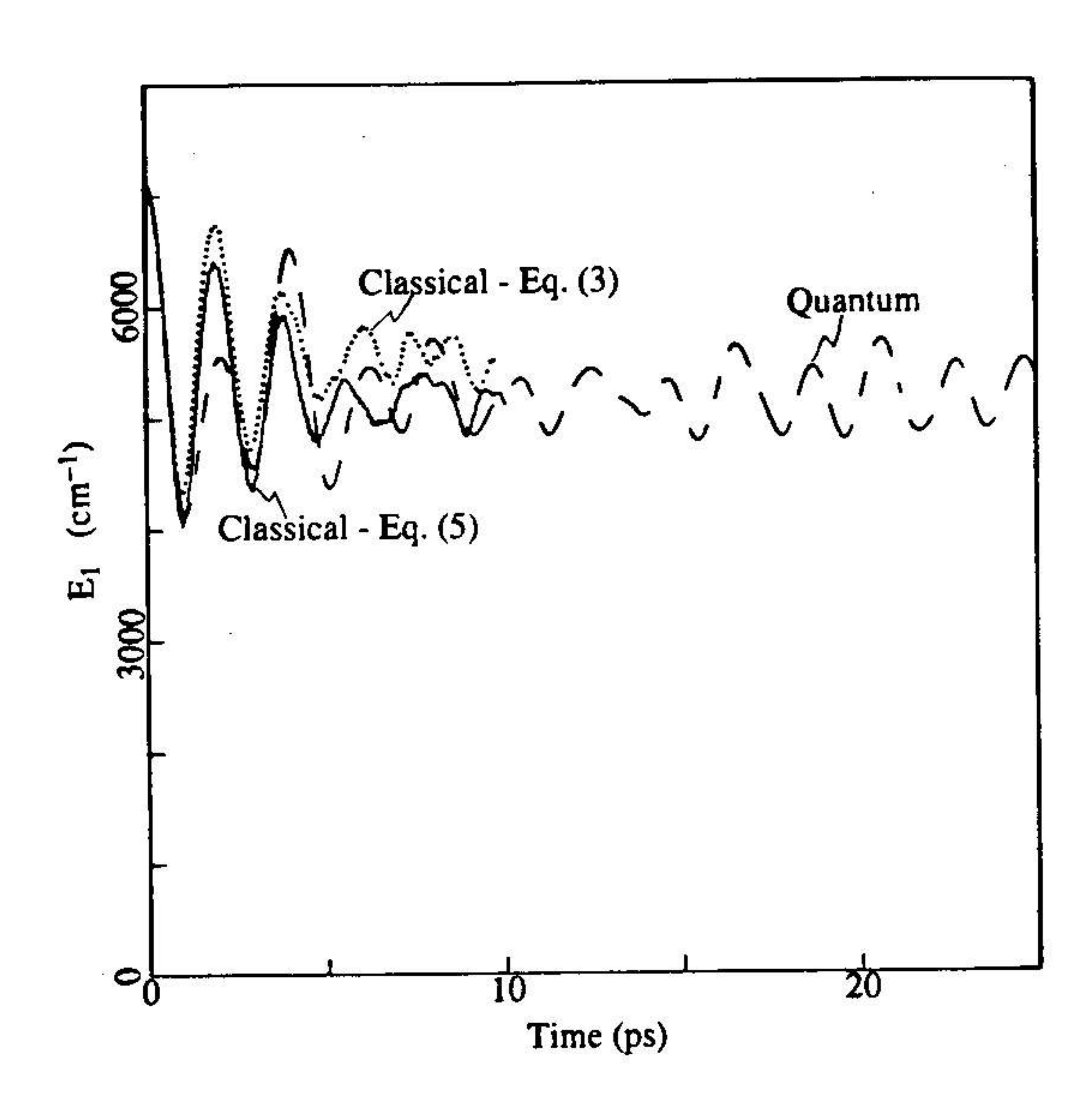


Fig. 8. Same as fig. 7 for the Sn (0, 15) state.

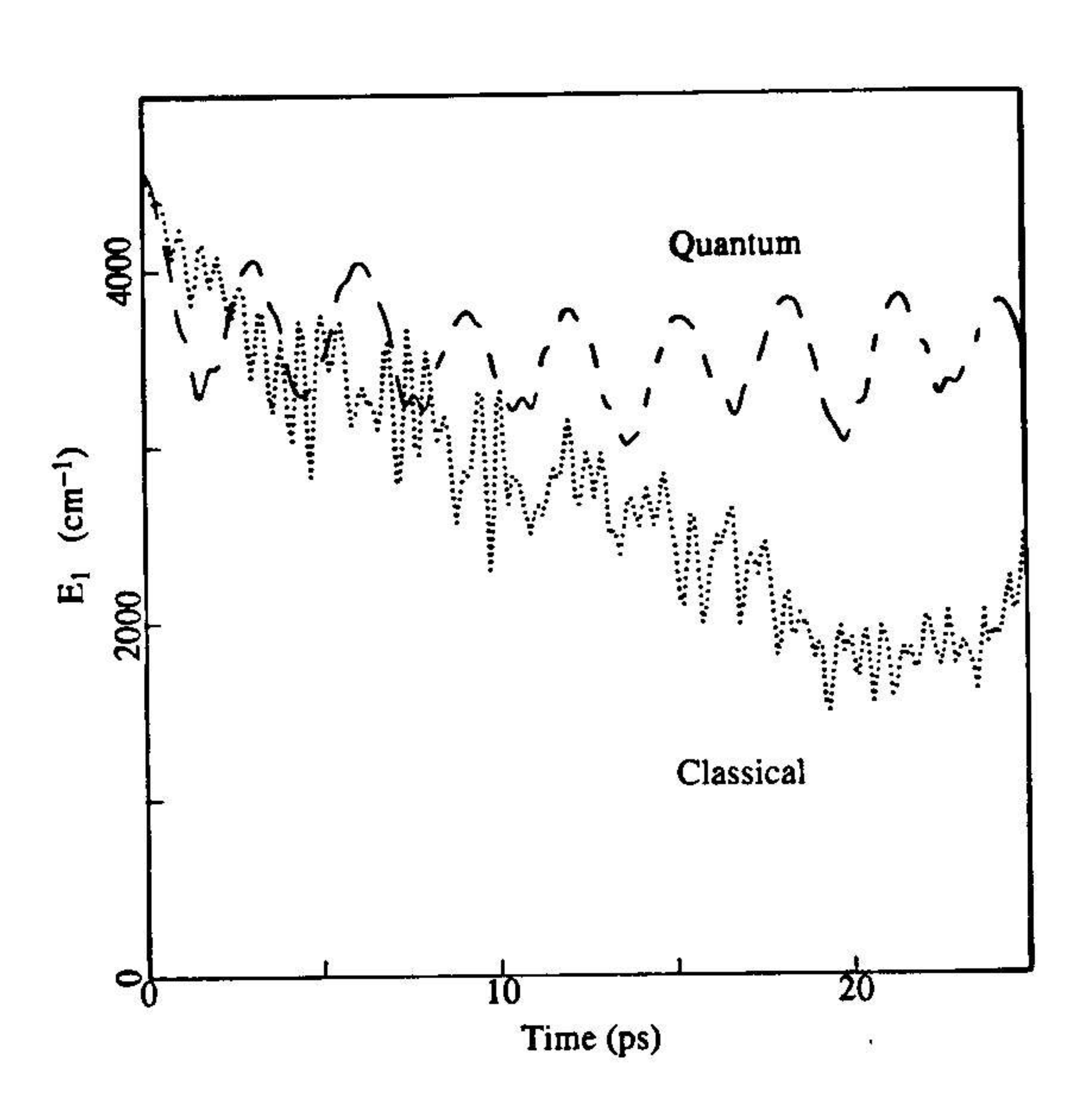


Fig. 9. Comparison of the quantum and classical calculation for the C(5,0) local group mode when the central mass is that of Si, where the greatest disagreement occurred between the quantum and classical calculations. The energy E_1 in L_1 is plotted versus time. The dashed line refers to the quantum calculation and the dotted line to the classical calculation using the Hamiltonian in eq. (3).

5. Discussion

In the model employed in this paper we have studied quantum mechanically an asymmetric, high-dimensional system which extends the study of the simpler (symmetric) models studied in refs. [1-3]. The dynamics found for this system are now probably due to the presence of multiple resonances and not to the single resonances responsible for the dynamics in the previous symmetric model systems. The multiple resonances in this asymmetric model would arise from the presence of a larger number of degrees of freedom. The present eleven-degree-of-freedom model led to a substantially larger density of states whose quantum dynamics could be modeled through the use of the artificial intelligence best-first search method. The present model also included the first derivative of the G matrix which included anharmonicities in the dynamics and served to couple the A' modes and the A modes of the model system. The anharmonicities were added in this way in the absence of detailed information on the other potential energy anharmonicities.

In the results presented in fig. 2 the difference in the dynamics for the C and Sn local group modes are shown for a similar energy of excitation. They are representative of the general trends observed throughout the calculations, where a greater relaxation of energy occurs for the Sn local group mode. This result is similar to the separability of the two modes, found in the previous symmetric models, but is now found to exist in a system with multiple resonances and more complex dynamics.

In figs. 3 and 4 results are given for the effect of the energy of excitation on the dynamics of the Sn and C local group modes. The dynamics given in fig. 3 shows that the amount of relaxation increases for the Sn local group mode when the energy of excitation is increased, whereas the amount of relaxation is near zero for all C local group mode excitations studied here. In fig. 4, the percent relaxation as a function of energy is plotted for the results in fig. 3. This quantitative plot confirms the trends seen in fig. 3 and shows that the amount of relaxation increases as a function of the excess energy of excitation for the Sn local group mode. This result is consistent with statistical models, which show a similar trend because the density of states increases exponentially as a function of the excess energy.

In contrast, the C local group modes show almost no relaxation for any of the energies of excitation. The lowest energy C local group mode excitation studied, the (4, 0) state, shows a percent relaxation comparable to the Sn local group mode with similar energy. This result, which is in contrast to the other C local group mode excitations, remains to be analyzed further. Also, the two C local group mode excitations presented for the (6, 0) state were used, because a unique identification of this state was not made using the primitive semiclassical quantization. This situation may have arisen from the presence of a resonance, and these two points represent a mixture of two nearby states and so may not be "pure" C modes. An exact description could have been made using the best of these two eigenfunctions of L_1 , but we did not analyze this point further.

In the results the effect of varying the mass (more precisely, the λ parameter) is shown in fig. 5 for the M (0, 8) and the C (5, 0) local group modes. For both types of excitation, the trend is for greater relaxation with decreasing central mass, with the Sn local group mode showing greater relaxation than the Clocal group mode. This result is expected intuitively, since the lighter central atom acts as a smaller barrier against energy transfer. A quantitative measure is given in fig. 6 where the percent relaxation is plotted versus λ for the results in fig. 5. (λ is proportional to the inverse of the mass and thus directly proportional to the coupling across the central atom.) The results shown confirm the trends seen in fig. 5 and show that the percent relaxation has a general linear dependence on λ . The C mode excitation for Ti ($\lambda = 2.4779$) does clearly not obey the trend of the other points. The reason for this exception was not explored further.

Some results for the comparison of the quantum and classical dynamics are given in figs. 7–9. In figs. 7 and 8 are results which are typical for many cases in which there was good agreement between the classical and quantum calculations. We first consider these results. In fig. 7 the result is depicted for the central mass of Sn for the (8, 0) C local group mode excitation. There is seen to be quantitative agreement at the shorter times, and no qualitative difference at longer times, between the classical and quantum results. Two different classical results are given, one which includes the first derivative of the G ma-

trix (eq. (3)) and the other which utilizes the full G matrix (eq. (5)). (Only the first derivative is used in the quantum results.) It is seen that no noticeable difference exists between the classical results for the first derivative and those for the full G matrix in this case, though the latter involved one order of magnitude more computer time than the former.

Results for the central mass of Sn for the (0, 15) Sn local group mode excitation are given in fig. 8. Here, there is a quantitative agreement at short times between the quantum and classical results. At longer times, the frequencies are in good agreement but the amplitudes only agree in their general trends. Further, as was the case in fig. 7, there are seen to be no qualitative differences between the classical results in the present study for the first derivative and those for the full G matrix. Since the use of the full G matrix in the quantum calculations is prohibitive for large systems, the agreement in the classical cases supports the use of the first derivative approximation to the full G

matrix in the quantum calculations. (This is especially true in light of the agreement between quantum and classical calculations.)

In fig. 9 the excitation used is the one having the largest disagreement and is typical of the case in which there was an appreciable difference in $E_1(t)$ between the classical and quantum results. In particular the frequencies in the classical results are seen to be quite different than the principal frequency in the quantum result. This type of disagreement was found only for the cases of the C local group mode (5, 0) excitation for the central masses of Si, Ti and Ge. For other excitations of the same central masses the disagreement was small and there was qualitative agreement (e.g., results for (0, 8) in table 2).

In table 2 the results are given for the percent relaxation for the classical, quantum, and statistical results for all excitations presented. For most cases there is good agreement between the classical and quantum results. The percent relaxation represents an av-

Table 2 Comparison of classical, quantum and statistical percent relaxation

Initial state (n_C, N_{Sn})	Excess energy (cm ⁻¹)	$R_{\%}$			
		classical	quantum	quantum $(t=\infty)$	statistical
Si (0, 8)	3855	47.2	48.5	52.8	74.2
Ti (0, 8)	3855	22.7	28.8	28.7	74.2
Ge (0, 8)	3855	17.2	21.0	23.2	74.2
Sn (0, 8)	3855	6.46	12.8	13.9	74.2
C: (5 A)	4574	42.7	22.7	22.2	75.3
Si (5, 0)	4574	41.5	39.0	37.0	75.3
Ti(5,0)	4574	11.9	4.8	6.9	75.3
Ge (5, 0) Sn (5, 0)	4574	1.22	0.18	0.88	75.3
C= (0 0)	3855	6.46	12.8	13.9	74.2
Sn (0, 8)	4796	9.66	15.4	15.5	75.5
Sn (0, 10)	5264	13.4	18.2	19.4	76.1
Sn (0, 11)	6191	21.8	22.9	25.3	76.9
Sn (0, 13) Sn (0, 15)	7109	21.8	26.2	34.4	77.5
C= (1 0)	3688	4.09	3.1	12.0	74.0
Sn (4, 0)	4574	1.22	0.18	0.88	75.3
Sn(5,0)	5445	0.25	1.4, 5.9	1.4, 6.0	76.2
$Sn(6,0)^{a}$	6300	0.23	0.01	0.01	76.9
Sn (7, 0) Sn (8, 0)	7141	0.13	0.0	0.0	77.5

a) The multiple values for the Sn (6, 0) for the quantum calculation are due to the two nearby states in the semiclassical quantization as noted in the text.

erage long-time behavior of the system and therefore does not represent the short-time agreement or the agreement in the frequencies at those times (e.g., figs. 7 and 8) which was typically present. The statistical estimate in table 2 of the percent relaxation is greater than that found in the dynamics calculations. This disagreement reflects the fact that the quantum calculations do not show equal probabilities for all states at long times. This result may be due to the lack of sufficient couplings and sufficient number of degrees of freedom to accurately model a large molecule. In some experiments strictly statistical results have been found, even at low energies [12]. A point of further study would involve the effect of including additional couplings and additional degrees of freedom, particularly in L₁, on the amount of relaxation present in the model system.

Thus, we have found that in most cases the classical estimate (with semiclassically chosen initial states) gives results at least qualitatively comparable to the quantum results at longer times and quantitative at shorter times. Such agreement illustrates the usefulness of classical mechanics in the present model system for the range of the various atoms considered and for the various frequencies involved and allows for the possibility of using classical mechanics in more complex models where the use of quantum mechanics may not be practical.

Acknowledgement

It is a pleasure to acknowledge the support of the US-Spain committee for Scientific and Technological Cooperation, the Fondo Nacional para el Desarrollo de la Investigación Científica y Técnica of Spain (Grant number PB85-0079), the National Science Foundation and the Office of Naval Research. We would also like to acknowledge the computing facilities at CIEMAT (Madrid).

Appendix

In this appendix we derive an expression for the percent relaxation in the limit of statistical distribution of energy in the present model system. In order to obtain an estimate of the statistical values for the

energy in L_1 or L_2 , a separability of the motions of L_1 and L_2 is assumed. With this approximation it is possible to define the density of states as a function of the excess energy for L_1 and L_2 , $\rho_1(\epsilon_1)$ and $\rho_2(\epsilon_2)$, respectively. When to every state of the system an equal probability is assigned, the resulting statistical value of the energy present in L_1 is given by the convolution integral [10],

$$E_{1}(E_{T}) = \int_{\epsilon=0}^{E_{T}} \rho_{1}(\epsilon) \rho_{2}(E_{T} - \epsilon) \epsilon \, d\epsilon$$

$$\times \left(\int_{\epsilon=0}^{E_{T}} \rho_{1}(\epsilon) \rho_{2}(E_{T} - \epsilon) \, d\epsilon \right)^{-1}, \qquad (A.1)$$

where E_T is the total excess energy in both L_1 and L_2 . In the semiclassical limit the density of states for a set of harmonic oscillators can be estimated by

$$\rho_1^{\text{sc}}(\epsilon_1) = (\epsilon_1 + E_{1,Z})^{S_1 - 1}$$

$$\times \left((S_1 - 1)! \prod_{i=1}^{S_1} h \nu_i \right)^{-1}, \qquad (A.2)$$

where $E_{1,Z}$ is the zero-point energy in L_1 , S_1 the number of degrees of freedom in L_1 and v_i the frequency of the *i*th harmonic oscillator in L_1 . An analogous expression applies for the $\rho_2^{\rm sc}(\epsilon_2)$. Using the fact that $S_1 = 2$ in the present model and after substitution of eq. (A.2) and the equivalent expression for $\rho_2^{\rm sc}(\epsilon_2)$ into eq. (A.1), one obtains

$$E_{1}^{\text{sc}}(E_{\text{T}}) = \left[\frac{2(E + E_{2,Z})^{S_{2}+2}}{(S_{2}+1)(S_{2}+2)} - \frac{E_{2,Z}^{S_{2}+1}}{S_{2}+1} \left(\frac{2E_{2,Z}}{S_{2}+2} + E_{\text{T}} + E_{1,Z} \right) + \frac{E_{1,Z}(E_{\text{T}} + E_{2,Z})^{S_{2}+1}}{S_{2}+1} - E_{\text{T}}E_{2,Z}^{S_{2}} \left(\frac{E_{2,Z}}{S_{2}+1} + E_{\text{T}} + E_{1,Z} \right) \right] / D, \qquad (A.3)$$

where

$$D = E_{1,Z} (E_{T} + E_{2,Z})^{S_{2}} + \frac{(E_{T} + E_{2,Z})^{S_{2}+1}}{S_{2}+1}$$
$$-E_{2,Z}^{S_{2}} \left(E_{T} + E_{1,Z} + \frac{E_{2,Z}}{S_{2}+1} \right).$$

The substitution of $E_1^{\rm sc}(E_{\rm T})$ into eq. (6) in the text for $\langle E_1 \rangle_{\infty}$ yields a statistical estimate for the percent relaxation. It can be easily shown that this expression for the percent relaxation approaches the expected limit of $100S_2/(S_2+2)$, i.e. the ratio of the number of degrees of freedom in L_2 to the total number of degrees of freedom, as $E_{\rm T} \rightarrow \infty$.

A more accurate estimation of the statistical value of $E_1(E_T)$ for the quantum case can be obtained by using the Whitten-Rabinovitch expression [18] for the density of states given by

$$\rho_{1}^{WR}(\epsilon_{1}) = (\epsilon_{1} + aE_{1,Z})^{S_{1}-1} \times \left((S_{1} - 1)! \prod_{i=1}^{S_{1}} h\nu_{i} \right)^{-1} \left(1 - \beta \frac{dw}{d\epsilon'_{1}} \right), \quad (A.4)$$

where

$$\epsilon'_{1} = \frac{\epsilon_{1}}{E_{1,Z}}, \quad a_{1} = 1 - \beta_{1} w_{1}(\epsilon'_{1}),$$

$$\beta_{1} = \frac{S_{1} - 1}{S_{1}} \frac{\langle v^{2} \rangle}{\langle v \rangle^{2}},$$

$$w_{1}(e'_{1}) = (5.00\epsilon'_{1} + 2.73\epsilon'_{1}^{0.5} + 3.51)^{-1} \quad \epsilon'_{1} < 1.0,$$

$$= \exp(-2.4191\epsilon'_{1}^{0.25}) \qquad 1.0 < \epsilon'_{1},$$

$$\frac{dw}{d\epsilon'_{1}} = -(5.00 + 1.365\epsilon'_{1}^{-0.5})w_{1}^{2} \quad \epsilon'_{1} < 1.0,$$

 $= (0.60478\epsilon_1')^{-0.75}w_1$ $1.0 < \epsilon_1'$

with an analogous formula for $\rho_2^{WR}(\epsilon_2)$. When these Whitten-Rabinovitch expressions are used in eq. (A.1), a numerical evaluation of the resulting expression was used to obtain a more accurate value of $E_1^{WR}(E_T)$. As expected the values obtained in both approximations show a larger disagreement at lower values of the total excess energy and approach the same asymptotic limit for infinite total excess energy. Eq. (A.4) was used in eq. (6) to obtain the statistical results in table 2.

Since harmonic estimates of the density of states were used in eq. (A.2) and the model presented contains anharmonic terms, it is useful to estimate the effect of anharmonicity on $E_1(E_T)$ in eq. (A.3). The maximum effect from anharmonicities on L_1 can be made by performing a Birge-Spöner fit to the C and Sn local group modes to obtain the value of the anharmonicity constant if they are presumed to be Morse oscillators. If the frequency for the anhar-

monic C and Sn local group modes is calculated with the Morse oscillator fit from the Birge-Spöner plot, where $E_{\rm T}$ is introduced for each mode, the lowest possible frequency for each mode is obtained for the L_1 modes. The use of these frequencies in eq. (A.2) for estimating $\rho_L^{\rm sc}(\epsilon_L)$ would give a maximum estimate of the density of states in L₁ and thus the minimum value of percent relaxation in eq. (6). It would represent a lower limit on the change of percent relaxation from the anharmonicity on L₁. The possible effect is small, as represented by the fact that the lower limit for percent relaxation for $E_T = 7027$ cm⁻¹ is 73.8, while utilizing eq. (A.3) gives 74.0. Thus, inclusion of the effect of the anharmonicity on L_1 in eq. (A.3) does not appreciably change the result. The effect of the anharmonicity in L₂ is not easily evaluated, but it is also presumed to be small, as was the case for L_1 .

References

- [1] V. López and R.A. Marcus, Chem. Phys. Letters 93 (1982) 232.
- [2] V. López, V. Fairén, S.M. Lederman and R.A. Marcus, J. Chem. Phys. 84 (1986) 5494.
- [3] S.M. Lederman, V. López, G.A. Voth and R.A. Marcus, Chem. Phys. Letters 124 (1986) 93.
- [4] P.J. Rogers, D.C. Montague, J.P. Frank, S.C. Tyler and F.S. Rowland, Chem. Phys. Letters 89 (1982) 9.
- [5] P.J. Rogers, J.I. Selco and F.S. Rowland, Chem. Phys. Letters 97 (1983) 313.
- [6] S.P. Wrigley and B.S. Rabinovitch, Chem. Phys. Letters 98 (1983) 386;S.P. Wrigley, D.A. Oswald and B.S. Rabinovitch, Chem.
 - Phys. Letters 104 (1984) 521.
- [7] K.N. Swamy and W.H. Hase, J. Chem. Phys. 82 (1985) 123.
- [8] C. Jaffé and P. Brumer, J. Chem. Phys. 73 (1980) 5646;
 R.T. Lawton and M.S. Child, Mol. Phys. 44 (1981) 709;
 E.L. Sibert III, W.P. Reinhardt and J.T. Hynes, J. Chem. Phys. 77 (1982) 3583, 3595;
 - T. Uzer and J.T. Hynes, NATO ASI Series C 200 (1987) 273.
 - Phys. Letters 146 (1988) 7; S.M. Lederman and R.A. Marcus, J. Chem. Phys. 88 (1988) 6312.

[9] S.M. Lederman, S.J. Klippenstein and R.A. Marcus, Chem.

- [10] P.J. Robinson and K.A. Holbrook, Unimolecular Reactions (Wiley-Interscience, New York, 1972).
- [11] E.B. Wilson, J.C. Decius and P.C. Cross, Molecular Vibrations (Dover, New York, 1955).
- [12] G.M. Stewart and J.D. McDonald, J. Chem. Phys. 78 (1983) 3907.

- [13] W.P. Neumann, The Organic Chemistry of Tin (Wiley, New York, 1970) p. 727.
- [14] J.R. Durig, Y.S. Li, J.F. Sullivan, J.S. Church and C.B. Bradley, J. Chem. Phys. 78 (1983) 1046.
- [15] C.R. Dillard and J.R. Lawson, J. Opt. Soc. Am. 50 (1960) 1271.
- [16] E.L. Sibert III, W.P. Reinhardt and J.T. Hynes, Chem. Phys. Letters 92 (1982) 455;
 - E.L. Sibert III, J.T. Hynes and W.P. Reinhardt, J. Phys. Chem. 87 (1983) 2032;
 - G.A. Voth, R.A. Marcus and A.H. Zewail, J. Chem. Phys. 81 (1984) 5494;

- W.H. Green, W.D. Lawrance and C.B. Moore, J. Chem. Phys. 86 (1987) 6000.
- [17] E.A. Solv'ev, Soviet Phys. JETP 48 (1978) 635;
 R.T. Skodje, F. Borondo and W.P. Reinhardt, J. Chem. Phys. 82 (1985) 4611;
 - B.R. Johnson, J. Chem. Phys. 83 (1985) 1204;
 - T.P. Grozdanov, S. Saini and H.S. Taylor, Phys. Rev. A 33 (1986) 55.
- [18] G.Z. Whitten and B.S. Rabinovitch, J. Chem. Phys. 38 (1963) 2466.